

## ANTIBIASING: HIGH MASS-TO-LIGHT RATIOS IN DENSE CLUSTERS

R. Brent Tully<sup>1</sup> and Edward J Shaya<sup>2</sup>

<sup>1</sup>*Institute for Astronomy, University of Hawaii  
2680 Woodlawn Dr., Honolulu, Hawaii, 96822, USA*

<sup>2</sup>*Hughes STX, Goddard Space Flight Center, Code 631  
Greenbelt, Maryland 20771, USA*

**ABSTRACT.** Modeling of the velocity field of the Local Supercluster leads to the conclusion that there must be a substantial differential between the mass-to-light ratios of most galaxies and those in a small number of special places. Specifically,  $M/L = 1000M_{\odot}/L_{\odot}$  is indicated for the full Virgo Cluster while  $M/L = 150M_{\odot}/L_{\odot}$  is appropriate for most environments. It is argued that a higher  $M/L$  value is characteristic of E/S0 knots, regions where the galaxy density is high and collapse time scales are short. Regions larger than galaxies where collapse is occurring only on the order of the age of the universe, the environment where spirals and irregulars predominate, are characterized by a low  $M/L$ . Overall, the mean density of the universe is well below closure. There could be comparable total mass in the relatively rare E/S0 knots as there is in the environments dominated by spirals and irregulars.

### 1 Introduction

The concept of ‘biasing’ arose out of a discussion by Kaiser (1984) that different classes of astronomical objects may trace the underlying mass distribution to greater or lesser degrees. It was appreciated, especially as comparisons were made with N-body simulations, that some fraction of mass could be only poorly correlated with the observable galaxies. A simple, perhaps simplistic, description is provided by the bias parameter of linear theory,  $b = \delta_g/\delta_m$ , where the *observed* galaxy fluctuation field is  $\delta_g$  and the mass density fluctuation field is  $\delta_m$ . The expectation has arisen from comparisons between models and the observed spectrum of irregularities (Davis et al. 1985) that mass would be more widely distributed than clusters and even field galaxies, so  $b > 1$ . In this case, it would be said that galaxies have a biased distribution compared with the mass.

While this sense of biasing may well occur, the focus of this paper is on the opposite possibility that matter may be more concentrated than light in some cosmologically important situations. At least locally, it could be that  $b < 1$ , a condition we will call ‘antibiasing’.

### 2 The Mean Density of the Universe

Dynamical studies of galaxy flows can give estimates of the mean density (Dekel 1994; Strauss & Willick 1995). There is a dichotomy of results. One method compares the divergence of the velocity field, which gives the mass density field, with some catalog of the observed distribution of galaxies. This method, called POTENT, gives values of  $\beta = \Omega_0^{0.6}/b$  that are indicative of a universe near closure density:  $\beta_I = 0.89 \pm 0.24$  (Sigad et al. 1998) and  $\beta_O = 0.74 \pm 0.26$  (Hudson et al. 1995) where the subscripts  $I$  and  $O$  indicate comparison with an Infrared Astronomy Satellite (IRAS) and optical catalog, respectively. Baker et al. (1998) find  $b_O/b_I \simeq 1.4$ , so these results would be compatible with  $\Omega_0 \sim 1$  and  $b_I \sim 1$ . The uncertainties are 95% confidence levels.

On the other hand, methods that compare expectation and observed velocities find lower values of  $\beta$ . Here, both linear and non-linear studies reach similar conclusions. The linear approximation is valid if  $\delta_m \lesssim 1$  (Peebles 1980):

$$\mathbf{v} = \frac{\beta}{4\pi} \int d^3 \mathbf{r}' \frac{\delta_g(\mathbf{r}')(\mathbf{r}' - \mathbf{r})}{|\mathbf{r}' - \mathbf{r}|^3}.$$

(1992) found  $\beta_O \lesssim 0.25$  ( $\beta_I \lesssim 0.35$ ), Reiss et al. (1997) found  $\beta_I = 0.4^{+0.3}_{-0.25}$ , da Costa et al. (1998) found  $\beta_I = 0.6 \pm 0.2$ , and Willick & Strauss (1998) found  $\beta_I = 0.50 \pm 0.10$ . A non-linear methodology we call ‘Least Action’ has been described by Peebles (1989, 1990, 1994, 1995) and Shaya, Peebles & Tully (1995). The non-linear studies determine, not  $\beta$ , but constraints on the parameter space ( $M/L, t_0$ ), where  $M/L$  is the conversion ratio from observed luminosities to mass and  $t_0$  is the age of the universe. The  $M/L$  values that are determined can be normalized by the mean luminosity density of the universe to constrain something equivalent to  $\beta$ . The results from our most recent analysis (Tully 1997) can be translated as  $\beta_O = 0.31 \pm 0.14$  ( $\beta_I = 0.43 \pm 0.20$ ). All the linear and non-linear studies that compare model velocities to observed velocities are in reasonable agreement and indicate that if  $\Omega_0 = 1$  then there needs to be considerable bias,  $b_I \sim 2$ .

### 3 Least Action

Shaya et al. (1995) describe our methodology for the reconstruction of the orbits of galaxies and groups using a variational principle. Tully (1997) gives updated results. Galaxies follow paths that extremize the ‘action’, the integral of the Lagrangian through time. In its simplest incarnation, the model can be restricted to only two free parameters. We have a catalog of galaxies within a velocity limit ( $3000 \text{ km s}^{-1}$ ) with known positions on the sky, redshifts, and luminosities, so one of our free parameters, the relation between mass and light ( $M/L$ ), specifies the mass associated with galaxies where they are today in redshift space. The other free parameter is the age of the universe,  $t_0$ , that specifies how long these masses have been tugging on each other. At the next level of complexity, a third parameter is added to take some account of biasing. A softening parameter is introduced to modify the force law so forces are reduced at close range to mimic the effects of inter-penetrating halos.

Once the three free parameters have been fixed, a Least Action re-enactment of the constituent orbits

gets all the galaxies to the right positions on the sky and the right redshifts (as boundary conditions) and specifies the other three elements of phase-space. The specification of model distances is what we care about because measured distances exist for  $\sim 1/3$  of the objects. A  $\chi^2$  evaluator is formulated to compare model and observed distance moduli,  $\mu_{m,i}$  and  $\mu_{o,i}$  respectively, for the  $i^{\text{th}}$  object:

$$\chi^2 = \sum_{i=1}^{N_\mu} w_i \left( \frac{(\mu_{o,i} - \mu_{m,i})}{\sigma_\mu} \right)^2 + \left( \frac{5 \log(cz_{o,i}/cz_{m,i})}{\sigma_\mu} \right)^2 / \sum_{i=1}^{N_\mu} w_i$$

Figure 1 illustrates the  $\chi^2$  values in the domain of the two principal free parameters ( $M/L, t_0$ ) with the softening parameter fixed at  $300 \text{ km s}^{-1}$ . (Note: since this model was created we have revised our table of distances; the Hubble Space Telescope observations of cepheids in external galaxies has resulted in a 10% upward revision of distances and ages: see Tully 1998). It can be seen that models with  $\Omega_0$  substantially less than unity are favored. Models with  $M/L \sim 200M_\odot/L_\odot$ ,  $t_0 \sim 10 \text{ Gyr}$  conform to observations.

### 4 The Virgo Cluster

Although the model described above provides a good description of the velocity field over most of the Local Supercluster, it fails miserably in one important region. A substantial infall pattern is observed around the Virgo Cluster but such a low value as  $M/L \sim 200M_\odot/L_\odot$  cannot explain the motions that are seen. It hardly helps to simply increase  $M/L$  for all objects. Doing so effectively increases the model  $\Omega_0$ , hence reduces  $t_0$  for a given distance scaling. There is then not enough time to build up the observed velocities. High global  $M/L$  cannot explain the infall velocities and the  $\chi^2$  figure of merit blows up.

The very strong conclusion is that we need a large *differential* in  $M/L$  between Virgo and most of the rest of the Local Supercluster. We need a modest  $M/L$  outside Virgo to get

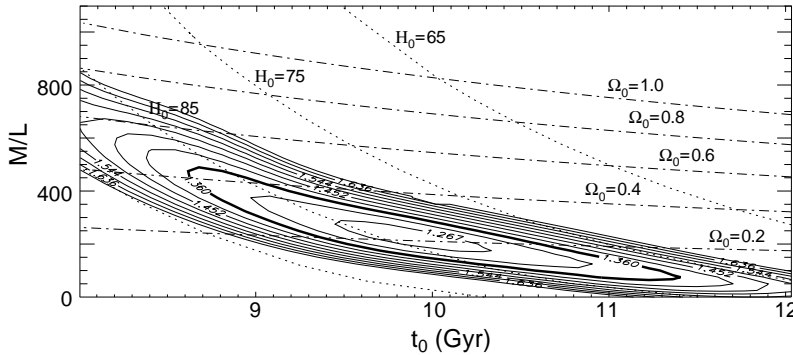


Figure 1. *Contours of  $\chi^2$  as a function of the two free parameters  $M/L$  and  $t_0$  with the force softening parameter set at  $300 \text{ km s}^{-1}$ . Contours at  $1\sigma$  intervals with the dark contour at the  $2\sigma$  level. This model is calibrated with distances that do not reflect a 10% increase in the zero-point resulting from recent cepheid distance determinations.*

a good  $\chi^2$  fit overall but we need a large  $M/L$  in the Virgo Cluster to explain the observed infall pattern.

Figure 2 illustrates the nature of our observational constraints. The group 11-4 (Tully 1987) is an entity in the Southern Extension of the Virgo Cluster, at an angle of  $9.3^\circ$  from the cluster center. The curves in each panel show the run of velocities with distance anticipated by two alternative models: on top, a model with  $\Omega_0 = 0.3$ ,  $M/L = 200M_\odot/L_\odot$  and, on the bottom, a model with  $\Omega_0 = 0.3$ ,  $M/L = 150M_\odot/L_\odot$  for most galaxies but  $M/L = 1000M_\odot/L_\odot$  for Virgo and a small number of other groups dominated by ellipticals and S0s. The points with error bars locate galaxies in group 11-4 with distance estimates. Clearly, the model that defines the curve in the top panel cannot explain the velocities that are observed. The model associated with the bottom panel does an adequate job.

All galaxies within the infall region can be considered in the same light. In each case, the run of velocities with distance along the pertinent line-of-sight can be calculated for any model. For a given  $t_0$ , there will be a threshold  $(M/L)_{\text{minimum}}$  that allows the observed velocity within the infall envelope.

It is helpful to appreciate that we do not need very precise distance estimates for this analysis. It is suffi-

cient to discriminate between three possibilities: is a galaxy to the foreground, within the infall region, or in the background? Since the Virgo multi-value region is seen to extend to  $\sim 25^\circ$  from the Virgo core, the infall region extends to  $\sim 1.2^m$  in front of the mean cluster distance and to  $\sim 0.8^m$  behind the mean distance. Our distance estimators are adequate to discriminate between the three alternatives. The case of Fig. 2 provides an illustration.

The Virgo Cluster caustic lies at  $\sim 6^\circ$  from the core and the infall is pronounced out to  $\sim 20^\circ$ . Within this annulus, we currently have 35 galaxies with distance determinations that unambiguously put them in the infall zone. These galaxies are falling in a quasi-laminar flow into the cluster. Figure 3 shows the constraints these galaxies provide for the same two models considered in Fig. 2. The circles show the observed velocities and angular distances from the cluster center of galaxies that are certified to be within the Virgo infall zone on the basis of distance measurements. The small open circles correspond to galaxies projected onto the cluster and, hence, are probable cluster members. The 35 filled circles correspond to galaxies projected outside the cluster proper. The horizontal bars in each panel indicate the maximum and minimum projected velocities along lines of sight to individual galaxies or groups of galax-

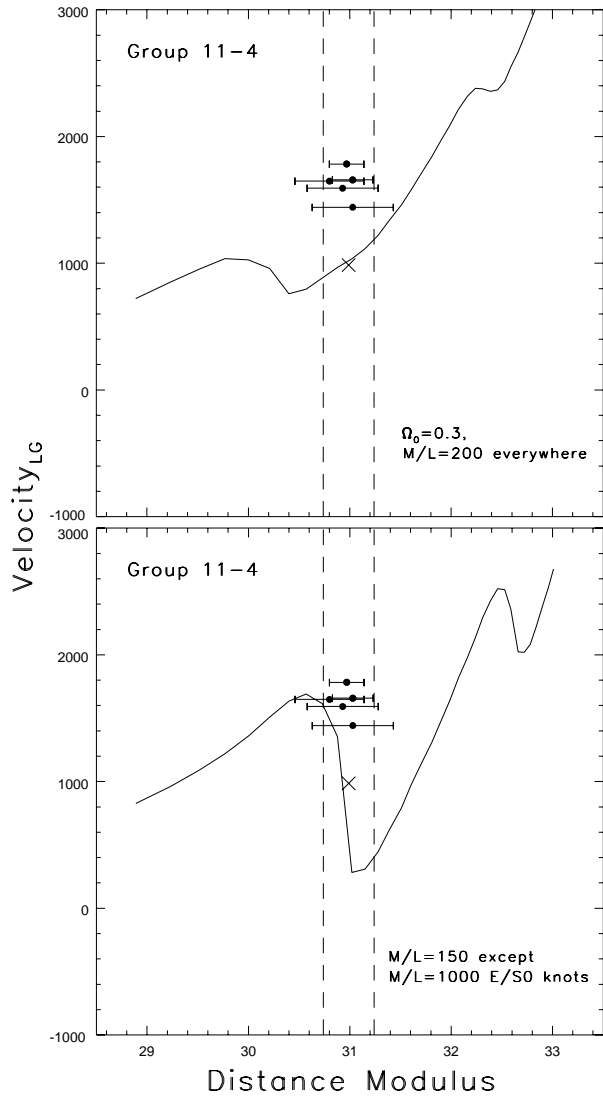


Figure 2. Example of model velocities along a line-of-sight close to the direction of the Virgo Cluster. In this case, the sight line is through Group 11-4. The points with errors correspond to galaxies in this group with distance determinations. The vertical dashed lines bracket the distance of the Virgo Cluster, centered in distance and velocity at the large cross. Top panel:  $M/L = 200$  for all entities. Bottom panel:  $M/L = 1000$  for Virgo and other E/S0 knots, otherwise  $M/L = 150$ . The second wave in the velocity curve beyond Virgo occurs because the line-of-sight passes near another E/S0 knot, the Virgo W Cluster, Group 11-24.

ies within the infall region. The 11-4 group used as an example above is at an angle of  $9.3^\circ$  and the maximum and minimum velocities anticipated by the single value  $M/L = 200M_\odot/L_\odot$  model (top panels Figs. 2 and 3) are  $1037$  and  $760$   $\text{km s}^{-1}$ , while the maximum and minimum velocities anticipated by the model with  $M/L = 1000M_\odot/L_\odot$  for Virgo,  $M/L = 150M_\odot/L_\odot$  for most other objects (bottom panels Figs. 2 and

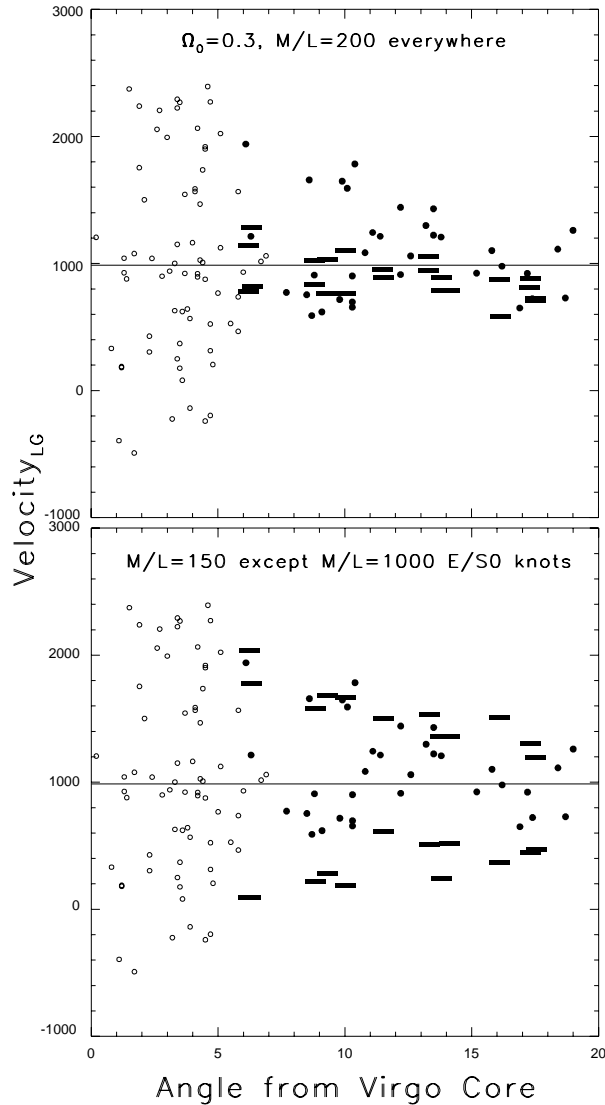


Figure 3. *Virgo infall constraints from two models. Horizontal bars are line-of-sight extrema velocities for a good overall  $M/L$  (top) and for a model with a lot of extra mass in Virgo (bottom).*

3) are 1690 and 283 km s<sup>-1</sup>. The model illustrated in the top panels totally fails to predict the observed infall pattern while the model displayed in the bottom panels is adequate. In this case, the Virgo Cluster is assigned  $1.3 \times 10^{15} M_\odot$ . This mass is higher than the Virial theorem mass of  $0.7 \times 10^{15} M_\odot$  (Tully & Shaya 1984), but the infall mass pertains to a scale  $\sim 3 \times$  larger than the Virial radius.

Fifteen years ago, Tully & Shaya

(1984) had already found this basic result that  $(M/L)_{virgo}$  has to be much higher than  $(M/L)_{field}$  in order to get a sensible infall description. That previous study was based on a fully non-linear but spherically symmetric model and one could wonder if the obvious departure of the observed galaxies from a spherical distribution in the Local Supercluster was affecting the solution. The present model provides a non-parametric description of the su-

percluster asymmetry (mass is distributed like the observed galaxies) and returns essentially the same answer. The infalling galaxies in Fig. 3 tend to have higher velocities than the cluster mean, partially a happenstance of uneven filling of the volume and partly due to angular momentum in the infalling population, naturally provided by the Least Action reconstruction. This velocity asymmetry was seen in the 1984 study but could not be described by the spherically symmetric model (see also Tully & Shaya 1994; Tully 1997).

### 5 High $M/L$ in a Small E/S0 Knot

Throughout the Local Supercluster there are places where the galaxy density is as high as in the core of the Virgo Cluster, though the total number of galaxies involved can be small. Usually in these cases the majority of the galaxies are ellipticals and S0s. There is some evidence that  $M/L$  values can be very high in these places. A dramatic case is the group around NGC 1407, Group 51-8 in our catalog (Tully 1987). Its unusual properties have been discussed by Gould (1993) and Quintana, Fouqué, & Way (1994). There are 19 galaxies with known redshifts associated with the group. Only NGC 1407 is an  $L^*$  galaxy. The second most luminous galaxy, NGC 1400, is more than three times fainter. All but one of the dozen that have been typed are E/S0/Sa. Quintana et al. find the velocity dispersion to be  $416^{+98}_{-58}$  km s $^{-1}$ , which gives  $(M/L)_{virial} = 600M_\odot/L_\odot$  after a tiny correction to our distance scale.

The S0 galaxy NGC 1400 deserves special attention. This galaxy is blueshifted by 1066 km s $^{-1}$  with respect to the group mean and would carry the vast majority of the kinetic energy of the group ( $\sim 85\%$  of the kinetic energy follows from the line-of-sight velocities). One way to rationalize this unusual situation is to suppose that NGC 1400 and the other galaxies carry only a small fraction of the mass of the gravitational potential well.

### 6 Other E/S0 Knots in the Local Supercluster

In a complete volume-limited sample in our vicinity of the Local Supercluster (extending to  $25h_{75}^{-1}$  Mpc with distances given by a model with spherical Virgo infall), 69% of the galaxies, and 77% of the light in galaxies, are in 179 groups (Tully 1987). Spiral and irregular galaxies predominate in the overwhelming majority of these groups. In these most common cases, the E/S0 representation is inevitably less than 20%, 1-dimensional group velocity dispersions are  $\sim 100$  km s $^{-1}$ , and group crossing-times are  $\sim 40\%$  of the Hubble time. However, eight of these groups are quite distinct. Indeed, they are among the best known nearby groups because of their compact nature. In these eight cases, *more than half of the galaxies are E/S0*. These early type galaxies are inevitably restricted to volumes only a few hundred kpc across. The groups usually have higher velocity dispersions than their spiral-dominated counterparts and crossing times are  $\lesssim 10\%$  of the Hubble time. The distinction between spiral-rich and E/S0-rich groups is quite pronounced, obscured only partially by the not-infrequent incidence of spirals at the periphery of E/S0 knots.

Table 1 provides a list of the complete sample of nearby groups dominated by elliptical and S0 galaxies (the asterisk in the final column indicates inclusion in the complete sample), plus a few other such groups at greater distances but still within 3000 km s $^{-1}$ . The most luminous and the faintest groups on the list have already been discussed. The Virgo Cluster and the NGC 1407 Group span a range from two dozen  $L^*$  galaxies and  $10^{15}M_\odot$  to a single  $L^*$  galaxy and  $2 \times 10^{13}M_\odot$ . Fornax, Coma I, Antlia, and NGC 1566 all have internal velocity dispersions that hint at large  $M/L$  values (Tully 1987).

### 7 Summary

The evidence for large  $M/L$  variations comes from combining two distinct sources of dynamical information. On the one hand, the Least Ac-

Table 1. *E/S0 Knots within 3000 km s<sup>-1</sup>*

| Name     | Catalog | $V_{LG}$ | Log $L_B$ |   |
|----------|---------|----------|-----------|---|
| Virgo    | 11 -1   | 986      | 12.14     | * |
| Fornax   | 51 -1   | 1466     | 11.52     | * |
| Virgo W  | 11-24   | 2225     | 11.43     |   |
| Coma I   | 14 -1   | 983      | 11.34     | * |
| NGC 5044 | 11-31   | 2559     | 11.19     |   |
| Antlia   | 31 -2   | 2519     | 11.12     |   |
| Eridanus | 51 -4   | 1415     | 11.06     | * |
| NGC 1566 | 53 -1   | 1076     | 11.03     | * |
| NGC 4125 | 12 -5   | 1436     | 11.00     | * |
| NGC 5846 | 41 -1   | 1810     | 10.99     |   |
| Leo      | 15 -1   | 722      | 10.73     | * |
| NGC 1407 | 51 -8   | 1522     | 10.58     | * |

tion reconstruction of orbits is telling us that most of the galaxies (ie, the spirals and irregulars) live in an environment with a modest mean density. On the other hand, the large infall motions into the Virgo Cluster and the large internal dispersions in other E/S0 knots are indications of a lot of mass in these special locations. The Least Action dynamical measurements encompass larger scales than virial measurements of internal group motions which probably explains why the Least Action mass estimates are larger by up to a factor 2. It is suggested that  $M/L \sim 150M_\odot/L_\odot$  for most galaxy associations but  $M/L \sim 1000M_\odot/L_\odot$  in the knots of ellipticals and S0s. Weak lensing provides a probe of the distribution of matter on supercluster scales for distant objects and it is interesting that hints are arising from that work that mass is strongly ‘antibiased’ toward the clusters (Kaiser et al. 1998).

If E/S0 knots do have much higher  $M/L$  values than galaxies in lower density regions there are several potential astrophysical explanations: (i) dimming at  $L_B$  is anticipated for older stellar populations, (ii) stripping from encounters might shred a large fraction of stars into intracluster space; Mendez et al. (1997) and Ferguson et al. (1998) find enough intracluster planetary nebulae and red giants between the galaxies in Virgo to indicate that there are comparable numbers of stars outside galaxies as in, (iii) dwarf spheroidal galaxies are found in large numbers in

Virgo (Phillipps et al. 1998) and Fornax (Ferguson & Sandage 1988) but evidently *not* in large numbers in Ursa Major or the field (Trentham, Tully, & Verheijen, in preparation) (iv) field galaxies may continue to accrete gas even until today, gas that gets converted into stars, while gas that arrives in clusters after the initial collapse of the cluster is outside the Roche-limit of individual galaxies and becomes virialized as hot gas in the intracluster medium (Shaya & Tully 1984). It is easy to entertain that most or all these effects occur and cumulatively could account for an  $M/L$  differential of the observed factor of 6-7.

Roughly 8% of the  $B$  light within 3000 km s<sup>-1</sup> comes from the galaxies associated with E/S0 knots. However, with the  $M/L$  differential that has been suggested, the E/S0 knots could contain  $\sim 40\%$  of the mass directly associated with galaxies. If so, there is a dramatic *antibiasing* of matter compared with IRAS-selected galaxies or even optically selected galaxies. Dark matter is more concentrated in a few places but enough so that it would have a cosmological impact. In addition, there may also be the *bias* of some matter poorly correlated with galaxies. The Least Action modeling strongly suggests that the overall density of matter is modest,  $\Omega_0 \sim 0.25$ . The POTENT observations of  $\Omega_0 = (b\beta)^{1.7}$  can be reconciled with a value of  $\Omega_0$  well less than unity if, overall,  $b_I < 1$ .

### Acknowledgments

We thank our close collaborator in this research, Jim Peebles.

### References

Baker, J.E., Davis, M., Strauss, M.A., Lahav, O., & Santiago, B.X., 1998, astro-ph/9802173

da Costa, L.N., Nusser, A., Freudling, W., Giovanelli, R., Haynes, M.P., Salzer, J.J., & Wegner, G., 1998, MNRAS, 299, 425

Davis, M., Efstathiou, G., Frenk, C.S., & White, S.D.M., 1985, ApJ, 292, 371

Dekel, A., 1994, Ann. Rev. Astron. Astrophys., 32, 371

Ferguson, H. C., & Sandage, A., 1988, AJ, 96, 1520

Ferguson, H.C., Tanvir, N.R., & von Hippel, T., 1998, Nature, 391, 461

Gould, A., 1993, ApJ, 403, 37

Hudson, M.J., Dekel, A., Courteau, S., Faber, S.M., & Willick, J.A., 1995, MNRAS, 274, 305

Kaiser, N., 1984, ApJ, 284, L9

Kaiser, N., Wilson, G., Luppino, G., Kofman, L., Gioia, I., Metzger, M., & Dahle, H., 1998, astro-ph/9809268

Mendez, R.H., Guerrero, M.A., Freeman, K.C., Arnaboldi, M. et al., ApJ, 491, L23

Peebles, P.J.E., 1980, The Large-Scale Structure of the Universe. Princeton University Press, Princeton

Peebles, P.J.E., 1989, ApJ, 344, L53

Peebles, P.J.E., 1990, ApJ, 362, 1

Peebles, P.J.E., 1994, ApJ, 429, 43

Peebles, P.J.E., 1995, ApJ, 449, 52

Phillipps, S., Parker, Q.A., Schwartzenberg, J.M., & Jones, J.B., 1998, ApJ, 493, L59

Quintana, H., Fouqué, P., & Way, M.J., 1994, A&A, 283, 722

Riess, A.G., Davis, M., Baker, J., & Kirshner, R.P., 1997, ApJ, 488, L1

Sigad, Y., Eldar, A., Dekel, A., Strauss, M.A., & Yahil, A., 1998, ApJ, 495, 516

Shaya, E.J., Peebles, P.J.E., & Tully, R.B., 1995, ApJ, 454, 15

Shaya, E.J., & Tully, R.B., 1984, ApJ, 281, 56

Shaya, E.J., Tully, R.B., & Pierce, M.J., 1992, ApJ, 391, 16

Strauss, M.A., & Willick, J., 1995, *Physics Reports*, 261, 271

Tully, R.B., 1987, ApJ, 321, 280

Tully, R.B., 1997, in Sato, K. ed., IAU Symp. 183, Cosmological Parameters and Evolution of the Universe. Kluwer Acad. Publ., Dordrecht

Tully, R.B. 1998, in Caputo, F. and Heck, A. eds., Post-Hipparcos Cosmic Candles. Kluwer Acad. Publ., Dordrecht. astro-ph/9809394

Tully, R.B., & Shaya, E.J., 1984, ApJ, 281, 31

Tully, R.B., & Shaya, E.J., 1994, in Durret, F., Measure, A., & Tran Thanh Van, J. eds., Clusters of Galaxies: Rencontre de Moriond. Editions Frontieres, Gif-sur-Yvette, p53

Willick, J.A., & Strauss, M.A., 1998, astro-ph/9801307